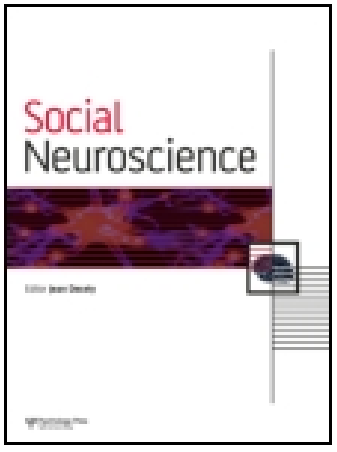

Social Neuroscience
Publication details, including instructions for authors and subscription information:
http://www.tandfonline.com/loi/psns20

The processes leading to deception: ERP spatiotemporal principal component analysis and source analysis

Shi-Yue Sun [a b], Xiaoqin Mai [c], Chao Liu [a c], Jia-Yan Liu [b] & Yue-Jia Luo [a]

[a] State Key Laboratory of Cognitive Neuroscience and Learning, Beijing Normal University, Beijing, China

[b] Institute of Psychology, Chinese Academy of Sciences, Beijing, China

[c] Center for Human Growth and Development, University of Michigan, Ann Arbor, MI, USA

Published online: 10 Jan 2011.

To cite this article: Shi-Yue Sun, Xiaoqin Mai, Chao Liu, Jia-Yan Liu & Yue-Jia Luo (2011) The processes leading to deception: ERP spatiotemporal principal component analysis and source analysis, Social Neuroscience, 6:4, 348-359, DOI: 10.1080/17470919.2010.544135

To link to this article: http://dx.doi.org/10.1080/17470919.2010.544135

SOCIAL NEUROSCIENCE, 2011, 6 (4), 348–359

Psychology Press
Taylor & Francis Group

The processes leading to deception: ERP spatiotemporal principal component analysis and source analysis

Shi-Yue Sun[1,2], Xiaoqin Mai[3], Chao Liu[1,3], Jia-Yan Liu[2], and Yue-Jia Luo[1]

[1]State Key Laboratory of Cognitive Neuroscience and Learning, Beijing Normal University, Beijing, China
[2]Institute of Psychology, Chinese Academy of Sciences, Beijing, China
[3]Center for Human Growth and Development, University of Michigan, Ann Arbor, MI, USA

The cognitive and neural mechanisms leading to deception were studied by the event-related brain potential (ERP) technique. In a simulated deception situation with graded monetary incentives, participants made a decision to lie or be truthful in each trial and held their response until a delayed imperative signal was presented. Spatiotemporal principal component analysis (PCA) and source analysis revealed that brain activities dominant in the left lateral frontal area approximately 800–1,000 ms post-stimulus and over the central-frontal-parietal and right frontal areas after 1,300 ms were significantly more negative in the deceptive condition than in the truthful condition. These results suggest that two serial cognitive processes, decision making and response preparation, are related to deliberate deception.

Keywords: Deception; Event-related brain potential (ERP); Stakes; Decision making; Response preparation; Principal component analysis; Source analysis.

Deception is a commonly observed phenomenon of social interaction. From the perspectives of evolutionary and developmental psychology, deception is a vital skill (Byrne & Corp, 2004; Ford, King, & Hollender, 1988; Hala & Russell, 2001; Lewis, Stanger, & Sullivan, 1989; Stromwall, Granhag, & Landstrom, 2007), socially undesirable but normal (Spence, 2004; Spence et al., 2004). In a cognitive framework, deception is a complex cognitive activity involving multiple processes, which has been defined as a deliberate attempt to mislead others (DePaulo et al., 2003; Vrij & Mann, 2001).

The activation-decision-construction model (ADCM) posits three cognitive processes underlying deception: activation, decision, and construction (Walczyk, Roper, Seemann, & Humphrey, 2003). When a question is asked, the true answer is loaded in working memory, and automatically becomes *active*. Since lies are usually related to factors such as self-interest, risk of being captured, and social context, the potential liar must evaluate these factors. Based on the evaluated information, the subject can then *decide* whether to honestly answer the question. Finally, the decision to lie guides the central executive of working

Correspondence should be addressed to: Yue-Jia Luo, State Key Laboratory of Cognitive Neuroscience and Learning, Beijing Normal University, 19 Xinjiekou Wai Street, Haidian District, Beijing 100875, P. R., China. E-mail: luoyj@bnu.edu.cn

This research was supported by the National Natural Science Foundation of China (30930031), Ministry of Science and Technology (973 Program, 2011CB711001; National Key Technologies R&D Program, 2009BAI77B01), and the Global Research Initiative Program, National Institutes of Health, USA (1R01TW007897). We thank J. Peter Rosenfeld for excellent suggestions regarding an earlier draft of this report and the PCA analysis. We also thank the two anonymous reviewers for their helpful comments. We are very grateful to Katy Mack Clark for her editorial assistance.

www.psypress.com/socialneuroscience DOI: 10.1080/17470919.2010.544135

memory. Lie *construction* quickly establishes an inhibitory link, which prevents utterance of the truth. Meanwhile, in an opposite direction, the social cognition context would suppress some potentially unsuccessful lies (Walczyk et al., 2003).

In the ADCM model, the automatic activation component is common to both truth-telling and lying; only the decision and construction contribute directly to deception (Walczyk et al., 2003). Consistent with the decision and construction components of the ADCM, Johnson and his colleagues divided the possible cognitive processes into two broad categories: those related to the intent or motivation for being deceptive and those related to making deceptive responses (Johnson, 2006; Johnson, Barnhardt, & Zhu, 2003). A neuroimaging study provided neural evidence for dissociable brain activities of the amygdala and prefrontal subregions in relation to these two different factors of deception (Abe, Suzuki, Mori, Itoh, & Fujii, 2007). Results from a delayed-answer test in a skin conduction response study to separate the intention to deceive from the act of deception suggest that it is the intention to deceive rather than the act of deception that is responsible for the differentiation-of-deception phenomenon (Furedy, Davis, & Gurevich, 1988).

Most previous studies have focused more on the act of deception than on its preparation and have emphasized the role of executive process in deception. For example, a series of ERP studies by Johnson and his colleagues suggested that two dissociable executive control processes contribute to deceptive responses: a tactical monitoring process that is used to overcome the prepotent truthful response and a strategic monitoring process invoked to keep track of the pattern of one's past truthful and deceptive responses (Johnson et al., 2003; Johnson, Barnhardt, & Zhu, 2004, 2005; Johnson, Henkell, Simon, & Zhu, 2008). Functional magnetic resonance imaging (fMRI) and positron emission tomography (PET) studies have revealed the activation of the prefrontal cortex (PFC) in deception processing (Abe et al., 2006, 2007, 2008; Ganis, Kosslyn, Stose, Thompson, & Yurgelun-Todd, 2003; Langleben et al., 2002, 2005; Lee et al., 2002, 2005, 2009; Spence et al., 2001; Spence, Kaylor-Hughes, Farrow, & Wilkinson, 2008). A meta-analysis across these results employing activation likelihood estimation quantitatively demonstrated that the deception-related regions including the bilateral ventrolateral PFC, dorsolateral PFC, anterior insula, and right anterior cingulate cortex overlap greatly with those found in executive function studies such as working memory, inhibitory control, and task switching (Buchsbaum, Greer, Chang, & Berman, 2005; Christ, Van Essen, Watson, Brubaker, & McDermott, 2009; Laird et al., 2005; Owen, McMillan, Laird, & Bullmore, 2005).

It remains unclear what is the temporal course of the decision or intention component of deception and the underlying neural correlates. A challenge to study the intention is that it is difficult to simulate a deception situation in which the participants deliberately and spontaneously deceive; that is, they might lie to gain a potential benefit or to avoid punishment, but without being explicitly instructed to lie (Sip, Roepstorff, McGregor, & Frith, 2008). In a megnetoencephalography study, Seth, Iversen, and Edelman (2006) made a breakthrough by developing a simulated customs setting in which the participants decided by themselves whether to lie by denying what they had or tell the truth by declaring the object. Truth-telling received a small but certain penalty, whereas lying involved both greater financial risk and greater potential reward. This is what happens in real-life deception, where there are always positive consequences of being believed and negative consequences of not being believed (Caso, Aldert, & Mann, 2005).

The purpose of the present study was to investigate the neural correlates of cognitive processes leading to deception, especially those related to the intention to deceive or preparation to deceive. We applied a "S1-S2" paradigm with a deception task similar to that of Seth et al. (2006). The participants were required to decide whether or not to lie after seeing the temptation stimulus (S1), but not to execute the response until seeing a subsequent imperative signal (S2). Therefore, the delayed responses made it possible to observe S1-related activities during the preparation stage, before the deceptive responses were executed (Fang, Liu, & Shen, 2003; Furedy et al., 1988). Meanwhile, the stake component was involved by rewarding the participants according to their lying performance. Participants believed that they would receive large gains if their lies were not being detected or they would face larger penalties if they were detected.

The contingent negative variation (CNV), a slow negative wave that is largest over central and frontal areas, is commonly found in the S1-S2 paradigm. It is widely accepted that the CNV consists of two separate components (for reviews, see Fabiani, Gratton, & Federmeier, 2007; van Boxtel & Böcker, 2004): an early initial CNV, reflecting the processing and evaluation of the warning signal (e.g., Weerts & Lang, 1973), and a late terminal CNV associated with motor preparatory processes and the anticipation of the imperative stimulus (Brunia & van Boxtel, 2001; Damen & Brunia, 1994; Leynes, Allen, & Marsh, 1998). Previous studies have found enhanced CNV in instructed deception (Fang et al., 2003). We expected

the same results would be obtained in the self-decided deception in the present study; that is, greater CNV before deceptive than before truthful responses.

METHODS

Participants

Nineteen right-handed undergraduates from the China Agricultural University (nine male, mean age of 20.9 years, range = 19–24) participated in this experiment. All of them had normal or corrected-to-normal vision and did not have any history of neurological or psychiatric disease.

Materials

Three pictures of a genuine Chinese RMB monetary bill (bank note) (US$1 ≈ 7 RMB) were used in this experiment. Each displayed a value of 1, 5, or 10 RMB. In addition, there was one fake RMB picture for each value marked by the serial number code "00000000." For example, the 5-RMB bill in Figure 1 was fake. All pictures were standardized to the size of 8×4 cm^2 (maximal visual angle = 4.6°) and a resolution of 72 pixels/inch, using Adobe Photoshop 7.0.

Deception task

A simulated "bill-identifying" task was used to induce deception. Participants were required to pick out the genuine RMB bill pictures from a set of mixed fake ones. They had to press the left key with their left index finger to report a genuine RMB and the right key with their right index finger to report a fake. The assignment of the "genuine" and "fake" responses to the two hands was balanced across participants. All participants were told that the purpose of the experiment was to test lie-detecting software. Therefore, for each genuine RMB bill, they could decide whether to "declare" it was genuine (i.e., tell the truth) or to "embezzle the money" by reporting it as fake (i.e., tell a lie). Telling the truth would gain them a small but certain monetary reward (+1% of the monetary value), whereas lying might lead to a larger potential gain (+100% of the value) if they were not caught by the software, but this carried the risk of a double penalty (–200% of the value) if they were caught. In fact, the feedback after the deceptive response was a 50/50 chance of gaining or losing money. The participants did not realize that the feedbacks were random until the experiment was finished and it was explained to them. They also learned that their final reward was the sum of their outcomes added to a basic compensation of 30 RMB (but not exceeding 60 RMB). In addition, the participants all knew that if they lied or told the truth all the time, the goal of examining the lie-detection ability of the software could not be achieved. Therefore, they were advised to make approximately equal deceptive and truthful responses to the genuine RMB bills.

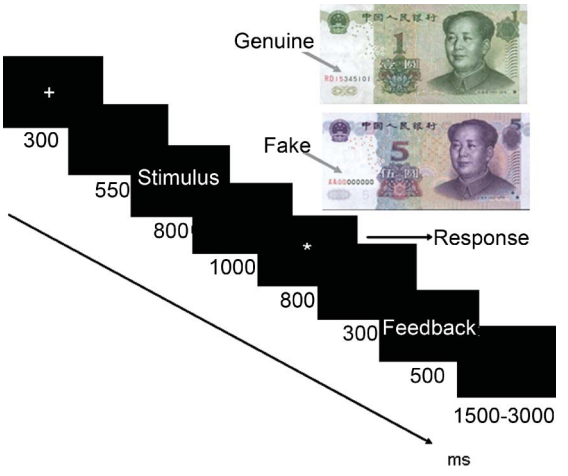

Figure 1. Experiment procedure for the spontaneous deception task, showing the trial format and example of genuine and fake RMB visual stimuli.

Additionally, those few fake RMB trials served as probes. The participants were instructed to respond truthfully to the fake bills because they would never benefit from lying about them. Feedback after a correct response to a fake bill was a visual message of "Good work," while if the participants responded incorrectly, they received a visual feedback of "Warning!" in red font. This operation aimed to avoid the participants responding arbitrarily to any bill, and thus it might increase task involvement. The data from the fake RMB trials were not analyzed further. However, if a participant's response accuracy to the fake bills did not exceed 90%, his or her whole data set was excluded.

The procedure is shown in Figure 1. The stimulus was a picture of an RMB bill (S1), genuine or fake, with a monetary value of 1, 5, or 10 RMB. The participants were instructed to decide on their response upon seeing each RMB picture but not to respond until the imperative signal (S2, an asterisk "*") was given. The "*" terminated at the response press or 800 ms after its onset if response latency was longer than 800 ms. The trials with response latency beyond 800 ms were excluded from data analysis. Then, after a

blank screen of 300 ms, feedback was presented. There was an interval of 1,500–3,000 ms between trials.

The experiment consisted of 360 trials with genuine RMB pictures and 72 trials with fake ones. Participants could take a rest every 36 trials. The total experimental duration was about 1 h, including a 10-min practice for participants to familiarize themselves with the procedure.

Electroencephalogram recording and data processing

Participants were seated in a dimly lit, electrically shielded, sound-attenuation chamber. The electroencephalogram (EEG) was recorded from 64 scalp sites with Ag/AgCl electrodes mounted in an elastic cap (NeuroScan, Inc., Herndon, VA, USA) according to the international 10/20 system. Participants were grounded with a forehead electrode. All EEG channels were referenced to the left mastoid, and were re-referenced off-line to the average of the left and right mastoids by subtracting from each sample of data recorded at each channel one-half the activity recorded at the right mastoid. Electrooculograms (EOG) were recorded bipolarly, both horizontally from electrodes at the outer canthi of the eyes and vertically from a pair of electrodes above and below the left eye. All electrode impedances were kept below 5 kΩ. The EEG and EOG were sampled at an A/D rate of 500 Hz/channel and a band-pass of 0.05–100 Hz.

Ocular artifacts were corrected in a regression procedure implemented by the NeuroScan software (Semlitsch, Anderer, Schuster, & Presslich, 1986). The EEG data were digitally low-pass filtered at below 30 Hz. ERPs were cut from 300 ms before the onset of RMB pictures to 2,200 ms after (with 300 ms pre-stimulus as baseline). Trials with amplitudes at any electrode greater than 100 μV or less than –100 μV were rejected to eliminate EOG and movement artifacts. The ERPs locked to RMB pictures followed by deceptive and truthful responses were separately averaged into two experiment conditions (deceptive/truthful). All averages were based on data from trials with genuine RMB pictures.

Spatiotemporal analyses and statistical analyses

A spatiotemporal principal component analysis (PCA), a theory-free and data-driven method, was conducted to determine the appropriate spatial sites and temporal epochs for estimating the effects of experiment manipulation (Spencer, Dien, & Donchin, 2001). The data sets came from the mean amplitude of each 10-ms time bin within the 0–2,200-ms window of all averaged ERPs and all subjects, which consisted of 62 scalp electrode sites × 220 time bins × 2 experimental conditions × number of subjects data (two EOG sites was excluded from the PCA). Both the spatial and temporal PCAs were based on the covariance between each pair of variables. Factors were extracted by the Varimax rotation procedure, with the criterion of eigenvalues greater than 1. As PCA results, the factor loadings represented the correlations between each electrode site and each corresponding factor. The factor score coefficients served as regression-like coefficients for weighting variables to estimate factor scores. First, a spatial PCA was performed, with the 62 electrode sites as variables and the 220 × 2 × 17 cases. The extracted principal spatial components can be considered as "virtual sites." Only those components accounting for 10% or more of the variance were entered into the following analysis. The factor scores of these spatial components were calculated by summing up the site amplitude values multiplied by the corresponding factor score coefficients. An original site was selected for computing a factor score only if its corresponding factor loading exceeded 0.7, and if its loadings on any other factors were less than 0.5. Then, temporal PCA was performed to reduce the temporal dimensionality of the time series of event-related spatial component factor scores at the "virtual sites." The factor scores of spatial components on each time bin became the variables (220), and the observations were virtual sites (number of the valid spatial components) × conditions × subjects. Within all the extracted principal temporal components, only those components accounting for 10% or more of the variance were selected as components of interest. The same principles as spatial PCA (i.e., main loadings greater than 0.70 and no cross-loadings greater than 0.50) were used to determine whether or not a time bin would contribute to calculating the factor score for a temporal component. Finally, the factor scores of each spatiotemporal component (e.g., the factor score of the first temporal component at the first "virtual site") were determined by summing the products of the spatial component factor scores of every chosen time bin and the corresponding factor score coefficients.

The scores of each spatiotemporal component were analyzed separately by multivariate repeated measures analysis of variance (MANOVA), in which the virtual sites were dependent variables. Response type (deceptive or truthful) was the independent

variable. Eta squared (η^2), a measure of effect size, was reported. If the main effect of response type reached significance, planned pairwise *t*-tests were performed to examine this effect. The spatial-temporal PCA and the MANOVA were both done with SPSS 15.0 (SPSS Inc., Chicago, IL, USA).

Source analyses

To estimate the cortical sources of scalp activity that are most relevant to the deceptive behavior, source analysis was performed on the grand average ERP under deceptive conditions, using the Brain Electrical Source Analysis program (BESA 5.0; Megis GmbH, Munich, Germany; Scherg & Ebersole, 1993). A four-shell ellipsoidal head model was used as an approximation for dipole fitting. The relative conductivities of the head model were set to 0.330 for brain, 0.330 for scalp, 0.042 for skull, and 1.00 for cerebrospinal fluid. Scalp and skull thickness were set to 6 and 7 mm, respectively.

The dipoles were fitted to the scalp amplitude topographies over specific time intervals (see Results section for details) for each of the aforementioned spatiotemporal components which showed deception differentiation. These intervals were chosen to minimize overlap among the adjacent components. Initially, PCA was employed to estimate the minimum number of dipoles that should be included in the model. The unseeded dipoles were started at arbitrary positions within the brain space. To maintain uniformity, all solutions were based on a central starting position. The orientation and strength of the dipoles were not restricted. Goodness-of-fit was estimated in terms of residual variance (RV). Then, another test dipole was added in order to ascertain that the number of dipoles in the models was sufficient. If a new dipole failed to improve the solution (e.g., it was fitted beyond the brain space, or its source activity did not reduce the RV), it was removed and the number of dipoles was determined to be sufficient. The resulting dipole positions were described in Talairach coordinates and projected onto a standardized structural MRI template.

RESULTS

Two participants were excluded from the analyses because they produced lying percentages in some stake situations less than 25% or more than 75%. This imbalance between truthful and deceptive responses meant that there were too few trials to generate ERP averages for the less-chosen responses. The data presented here were from the remaining 17 participants.

Pairwise *t*-tests revealed that the difference between the response times (RTs) after onset of S2 for the deceptive and for the truthful conditions was not significant ($p > .1$; 319 ± 16 ms and 322 ±15 ms for deceptive and truthful conditions, respectively). The mean RT for the fake condition was 304 ms (*SD* = 58 ms), which did not differ from the RT of either deceptive or truthful responses.

The percentages of participants' deceptive choices under the different values of the RMB were similar (47.5%, 52.7%, and 51.9% for 1, 5, and 10 RMB, respectively). The average response accuracy for the fake RMB was 97.5% (*SD* = 3%). There were 133 ± 51 and 119 ± 61 sweeps averaged for ERPs of deceptive and truthful conditions, respectively. Figure 2 shows the difference between the grand average ERPs of these two conditions.

Spatial PCA

The spatial PCA yielded six spatial factors, which explained 91.0% of the variance in spatial distribution. The spatial factor loadings were mapped to the scalp topography to show the distribution of the spatial components (Figure 3a). The first four factors (accumulatively accounting for 83.2% and each accounting for 10% or more of the variance), which separately reflected activity over the frontal-central-parietal, parietal-occipital, right lateral frontal, and left lateral frontal areas, went into further analysis. The spatial factor scores were computed by weighting the selected sites by the corresponding factor score coefficient matrix; that is, FC3, FCZ, C1, C2, C3, C4, CZ, CP1, CP2, CP3, CP4, and CPZ for the frontal-central-parietal region; P5, P6, P8, PO3, PO4, PO5, PO6, PO7, PO8, POZ, O1, O2, and OZ for the parietal-occipital region; FP2, AF4, AF8, F4, F6, F8, FT8, and FC6 for the right lateral frontal region; and FP1, AF3, AF7, F3, F5, F7, FT7, and FC5 for the left frontal region. The group averaged spatial factor scores for each condition are presented as ERPs at these four virtual sites (Figure 3b).

Temporal PCA

A temporal PCA was then performed on the four-virtual-site ERPs data. Twelve temporal components (temporal factors;TF) with eigenvalues greater than 1 were extracted, accounting for 95.6% of the temporal

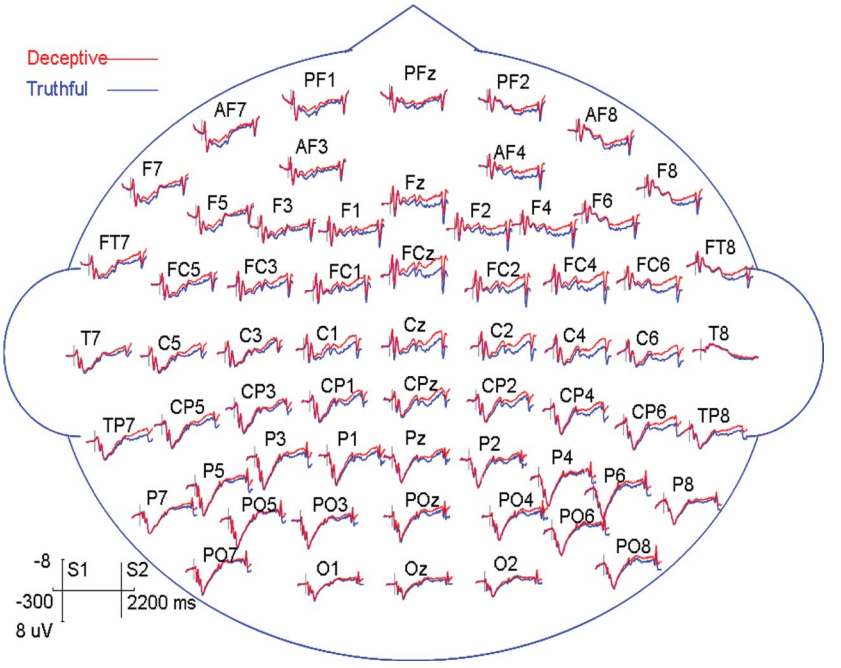

Figure 2. Grand average ERPs (62 scalp electrode sites) of deceptive and truthful conditions.

variance. We focused on the first three components, TF1, TF2, and TF3, because each of these components could explain more than 10% of the variance. Figure 3c shows the factor loadings of these components. The TF2 loaded highly around 450 ms, with the largest positive factor scores over the parietal-occipital regions. This might represent the brain activity associated with the late positive component. Considering that TF1 had the largest negative factor scores over the central areas and its factor loadings decreased after the onset of S2, TF1 could reflect the late part of CNV. TF3, whose loadings began to increase almost synchronously with TF1, is possibly associated with the initial subcomponent of CNV. Corresponding to the unique high loadings criterion, the representative time intervals for TF2, TF3, and TF1 were 300–650, 780–990, and 1,360–2,060 ms, respectively. The factor scores of these three spatiotemporal components for individual subjects were computed on each virtual-site ERP by summing the product of spatial component factor score in each time bin and the corresponding temporal factor score coefficient (Figure 4).

Statistical analyses

For each spatiotemporal component, MANOVA was conducted on the factor scores with the four virtual sites (i.e., the spatial components) as dependent variables.

300–650 ms

Neither the omnibus MANOVA nor the test on individual virtual sites showed a significant main effect of response type in this interval.

780–990 ms

The omnibus MANOVA did not indicate significant effect. While the univariate test showed that the effect of response type was significant over the left frontal area, $F(1, 16) = 11.02$, $MSE = 2.51$, $p < .005$, $\eta^2 = .41$, and over the frontal-central-parietal regions, $F(1, 16) = 5.56$, $MSE = 3.25$, $p < .05$, $\eta^2 = .26$, the planned *t*-test indicated that the spatiotemporal component factor score was more negative for the deceptive than the truthful condition (1.53 ± 0.70 vs. 3.34 ± 0.76 over the left frontal and -0.99 ± 0.77 vs. 0.47 ± 0.85 over the frontal-central-parietal areas).

1,360–2,060 ms

The omnibus MANOVA revealed no significant effects. The main effect of response type reached significance over the frontal-central-parietal and right frontal areas, $F(1, 16) = 8.06$, $MSE = 9.37$, $p < .05$, $\eta^2 = .24$, and $F(1, 16) = 7.82$, $MSE = 5.65$, $p < .05$, $\eta^2 = .33$, respectively. The spatiotemporal component factor scores were more negative for the deceptive than the truthful condition over these regions (-3.71 ± 1.47 vs. -0.73 ± 1.96 over the frontal-central-parietal areas

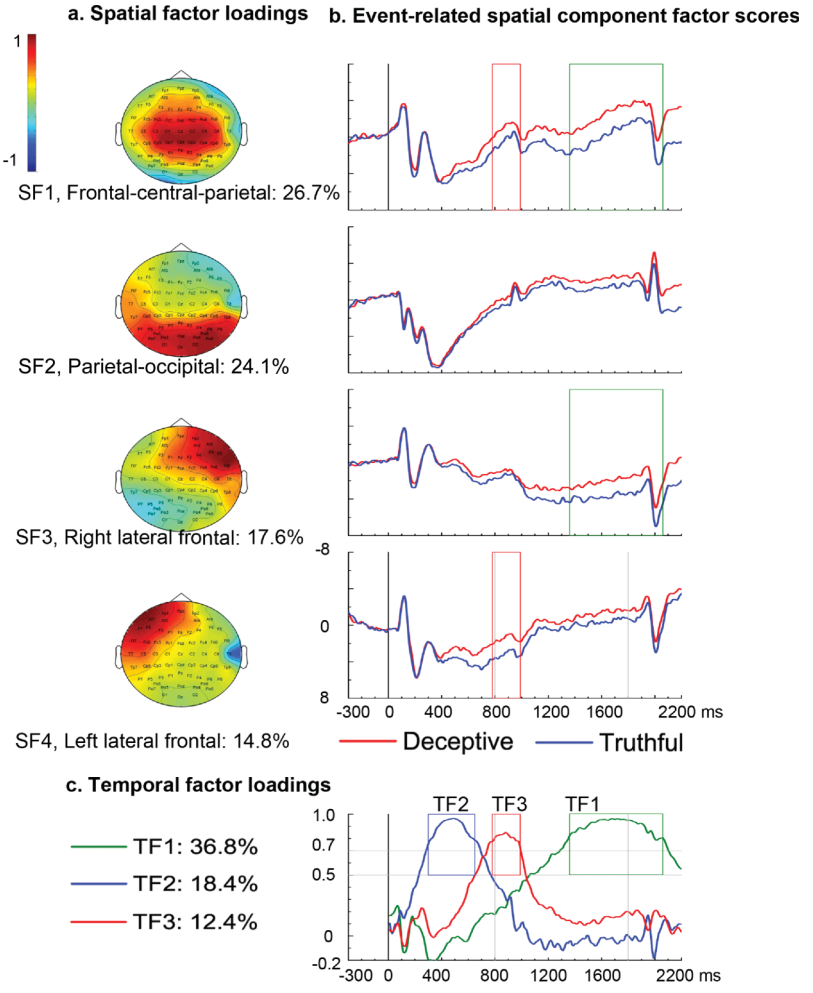

Figure 3. Brain activities revealed by the spatiotemporal PCA. (a) Topographic maps of the factor loadings for the first four spatial components. (b) Grand average spatial component factor scores in time series at these four spatial components (virtual sites). The value of the factor scores (y-axis) represents the brain activity, but not exactly the amplitudes. It is a unitless dimension. (c) The factor loadings of the first three spatiotemporal components in time series. The colored rectangles in (c) mark the time intervals with unique high loadings epochs for TF2, TF3, and TF1. The colored rectangles in (b) indicate significant main effects of response types of the MANOVA analysis ($p < .05$) on the corresponding spatiotemporal factors. The vertical line at the 0,800, and 1,800 ms on the time axis in (b) and (c) indicate the onset of S1, the offset of S1, and the onset of S2, respectively.

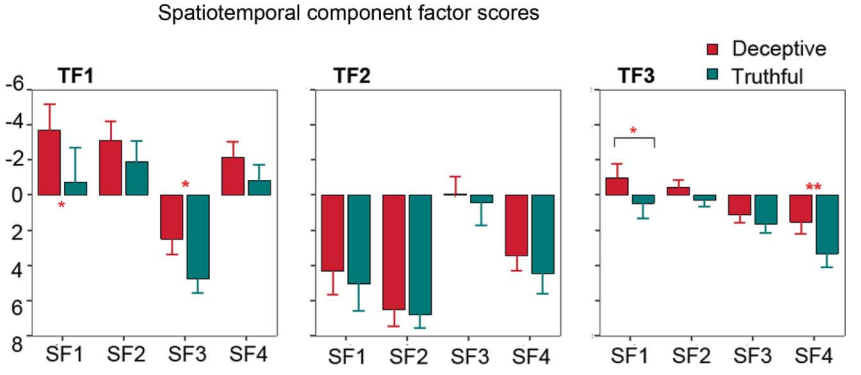

Figure 4. The factor scores of each spatiotemporal component. The red asterisk (*) indicates a significant difference between the deceptive and truthful conditions (*$p < .05$; **$p < .005$).

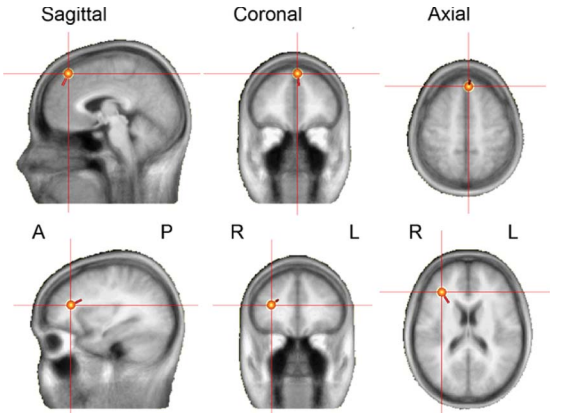

Figure 5. The dipole localizations of the grand averaged ERP in the deceptive condition in the time interval of TF3 (top panel) and TF1 (bottom panel). A: anterior; P: posterior; R: right; L: left.

and 2.51 ± 0.88 vs. 4.79 ± 0.79 over the right frontal areas).

Dipole locations

The identification of two distinct spatiotemporal components sensitive to the deception in the PCA, together with the high-density array of electrodes used here, supports the use of dipole source analysis to investigate the cortical sources of these components. For the earlier component, PCA decomposition of the 780–990 ms post-stimulus epoch indicated that one principal component could explain 95.5% of the variance in the data. Therefore, a single dipole model was fitted in this time interval. The result indicated that it was located in the left (near to midline) superior frontal gyrus (Talairach coordinates: x = –5, y = 37, z = 51, BA8; RV, 19.17%), downward oriented. For the later component, the time window of 1,350–2,000 ms was set as the interval of interest. One dipole accounted for 90.4% of the variance. It was located near the right frontal subgyral white matter, right inferior frontal gyrus, and right insula (Talairach coordinates: x = 33, y = 32, z = 18, RV, 23.28%). No more dipoles could be fitted in either time window, because other plausible alternatives, such as exploratory multiple dipole models, had resulted in locations beyond the brain space and thus did not improve these solutions. Figure 5 shows the calculated best-fit dipole positions for these two spatiotemporal components.

DISCUSSION

The aim of the present investigation was to identify the neural correlates of cognitive processes leading to deception, especially those occurring before the deceptive behavior takes place. Generally, real-life deception has two stages: the deliberation or intention on the part of the deceiver, and then the act of misleading others. Previous literature about the neural mechanisms of deception, including fMRI, PET, and ERP studies, has focused on the act of deception, and the results implicate the role of executive processes in deception, particularly working memory, conflict control, inhibition, monitoring, and task switching. However, although it is an important component of deception, deliberation or intention during the deceptive preparation stage has attracted little attention to date. In the few studies that examined the intention to lie, a PET study compared truth telling and lying with or without deceptive intentions and suggested the functional dissociable roles of the prefrontal subregions in making untruthful responses and the amygdala in deceiving others (Abe et al., 2007). In a similar ERP study, researchers found the same medial frontal negative deflection (N450) when participants lied and when they told the truth with deceptive intent (Carrión, Keenan, & Sebanz, 2009). In the present experimental paradigm, participants were left to decide by themselves whether to lie in each trial with the monetary incentives. Hence, the current manipulation should have captured, at least in part, the "deliberate" characteristic of deception.

As expected, the deception preparation is associated with overall greater negative deflection, consistent with the CNV results reported by Fang et al. (2003). There are both cognitive and emotional factors specifically related to deception that might enhance brain activity, including uncertainty about the deception outcomes, motivation and decision to lie, conflict control, prepotent response inhibition, strategic monitoring, fear and/or anxiety experiences, and possible countermeasures against detection.

Thanks to the spatiotemporal PCA, each temporal component could represent the ERP component with its "clean" shape by extracting and quantifying temporal components free of the influences of adjacent subcomponents. The two-stage deception preparation revealed by spatiotemporal PCA in the current study is in line with the interpretation that there are two crucial processes engaged in a lie's generation: decision making and response preparation (Johnson, 2006; Walczyk et al., 2003). Moreover, within the context of the ADCM model, there is an additional preceding activation process, which is automatic and common to both deception and truth telling (Walczyk et al., 2003). Consistent with this is the absence of a deception effect in the earlier component (around 300–700 ms) in our data. The temporal characteristic and scalp

distribution suggest that the brain activities in approximately 800–1,000 ms post-S1 and after 1,300 ms (500 ms pre-S2) could represent the initial CNV and the terminal CNV, respectively. This hypothesis is confirmed by previous research reports that initial CNV begins approximately 800 ms after the warning signal and that terminal CNV starts a few hundred milliseconds before the imperative stimulus (Damen & Brunia, 1994; Leynes et al., 1998).

The early deception differentiation in an approximately 800–1,000-ms interval might indicate the deceptive decision.

The decision to deceive is based on evaluation of reward and risk (Walczyk et al., 2003), because people usually lie to gain benefit or to avoid punishment, but they also take the risk of even greater loss or punishment (Caso et al., 2005; Seth et al., 2006). Therefore, possibly the decision and evaluation are inherently inseparable from the reward and/or risk processing. Thus, the enhanced early CNV (in the interval of around 800–1,000 ms) elicited by deception could be related to the heightened attention or emotion associated with the more risky choice and/or more meaningful reward following deception, and the anticipation of making an evaluative decision (Chiu, Ambady, & Deldin, 2004). In addition, sourcing analysis has revealed that the scalp activity at 800–1,000 ms was generated from the left superior frontal gyrus. Concordant with these spatial characteristics, studies suggest that damage to the left ventrolateral and orbital cortices impair reward evaluation and behavior flexibility in risk-taking decisions (Fellows & Farah, 2005; Floden, Alexander, Kubu, Katz, & Stuss, 2008). Functional imaging demonstrates a number of brain areas involved in the reward processing, including the PFC, parietal cortex, and subcortices such as the striatum, insula, and caudate (Knutson, Fong, Adams, Varner, & Hommer, 2001; Knutson, Fong, Bennett, Adams, & Hommer, 2003; Seymour, Daw, Dayan, Singer, & Dolan, 2007). Liu et al. (2007) have investigated reward anticipation in a monetary decision-making task. Although they have not explicitly discussed the functional hemispheric lateralization, the results revealed greater activation in the left superior frontal cortex and medial orbitofrontal cortex for the upcoming risky choice; i.e., choosing to bet rather than to bank money. Similar results of reward-sensitive activity in the left medial frontal gyrus are also found in the studies of Nieuwenhuis et al. (2005) and Fukui et al. (2005).

The terminal CNV represented by the activity at 1,350–2,000 ms is thought to be associated with the preparation of a signaled response and the simultaneous anticipation of the imperative stimulus (Brunia & van Boxtel, 2001; Verleger, Wauschkuhn, van der Lubbe, Jaskowski, & Trillenberg, 2000). The source analysis showed that the generator of scalp activity in this interval was located near the right inferior frontal gyrus, which has been proposed to be the functional location of response inhibition in previous brain injury studies (Aron, Robbins, & Poldrack, 2004; Clark et al., 2007; Clark, Manes, Antoun, Sahakian, & Robbins, 2003). In functional imaging studies with the Go/No-Go task, researchers have found activation in the bilateral prefrontal areas during the No-Go trials (Bellgrove, Hester, & Garavan, 2004; Fassbender et al., 2004; Liddle, Kiehl, & Smith, 2001), while other studies suggest the dominant role of the right prefrontal area, including the middle frontal gyrus and inferior frontal gyrus, in inhibitory control (Aron & Poldrack, 2006; Garavan, Ross, & Stein, 1999; Garavan, Ross, Murphy, Roche, & Stein, 2002; Konishi et al., 1999; Mostofsky et al., 2003). Therefore, the greater activity after 1,300 ms suggests that preparation for deceptive responses is more cognitively demanding in order to handle the additional cognitive processes such as inhibiting the prepotent truthful response.

As for behavioral performance, the current data revealed no difference between either deceptive and truthful responses or different stake conditions, and this finding is inconsistent with previous findings that deceptive responses produced longer latencies (Johnson et al., 2003, 2004, 2005, 2008; Walczyk et al., 2003). The delayed response in the present study may account for this inconsistency.

Despite our efforts to create a realistic deception task in which participants decided by themselves whether to lie and when to lie, the possibility remains that the deception in the laboratory may not absolutely imitate deception in real life. Firstly, the technical characteristics of the ERP methodology require an equitable number of averaged sweeps for ERPs in comparable conditions. In order to avoid participants' choice bias between deceptive and truthful responses, participants were advised to deceive on about half of the trials. This instruction, just as that in the random deception of Johnson et al. (2005), partially limited the absolute spontaneity of choices, though participants still had to decide whether to lie in each trial. Secondly, it is difficult to simulate the complex social factors and the emotional components inherent in real-life deception. Future studies addressing the cognitive and brain mechanisms underlying deception should consider the emotional and social aspects of deception.

In the current deception task and in the simulated customs setting of Seth et al. (2006), deception was

initiated at monetary temptation and involved both risk of losing money and greater potential gain. The advantage is that these tasks simulate both the causes and consequences of real-life deception. On the other side, it brings another limitation that we are not able to separate the deception from risk or reward processing. We could not rule out the possibility that the difference between deception and truth telling is due to different levels of reward and risk processing, because the deceptive choice was essentially riskier, and the related outcome was uncertain and subjectively more meaningful. Future studies with direct comparison between deceptive decision and economical risk-decision might help address this issue.

In summary, the greater activity associated with deception suggests that deception is more cognitively demanding than telling the truth. The spatiotemporal PCA and source analysis of the ERPs suggest neural correlates of two successive processes leading to the deliberate deception: decision making and response preparation. Decision making is an early process engaged in spontaneous deliberate deception. Potential liars decide to lie based on information evaluation. Response preparation is engaged later to inhibit the prepotent truthful response tendency, as well as to modulate other behavioral controls. These two separate preparative stages or processes appear to involve different localized brain activity.

Manuscript received 19 January 2010
Manuscript accepted 5 October 2010
First published online 10 January 2011

REFERENCES

Abe, N., Okuda, J., Suzuki, M., Sasaki, H., Matsuda, T., Mori, E., et al. (2008). Neural correlates of true memory, false memory, and deception. *Cerebral Cortex*, *18*(12), 2811–2819.

Abe, N., Suzuki, M., Mori, E., Itoh, M., & Fujii, T. (2007). Deceiving others: Distinct neural responses of the prefrontal cortex and amygdala in simple fabrication and deception with social interactions. *Journal of Cognitive Neuroscience*, *19*(2), 287–295.

Abe, N., Suzuki, M., Tsukiura, T., Mori, E., Yamaguchi, K., Itoh, M., et al. (2006). Dissociable roles of prefrontal and anterior cingulate cortices in deception. *Cerebral Cortex*, *16*(2), 192–199.

Aron, A., & Poldrack, R. (2006). Cortical and subcortical contributions to stop signal response inhibition: Role of the subthalamic nucleus. *Journal of Neuroscience*, *26*(9), 2424–2433.

Aron, A., Robbins, T., & Poldrack, R. (2004). Inhibition and the right inferior frontal cortex. *Trends in Cognitive Sciences*, *8*(4), 170–177.

Bellgrove, M., Hester, R., & Garavan, H. (2004). The functional neuroanatomical correlates of response variability: Evidence from a response inhibition task. *Neuropsychologia*, *42*(14), 1910–1916.

Brunia, C. H. M., & van Boxtel, G. J. M. (2001). Wait and see. *International Journal of Psychophysiology*, *43*(1), 59–75.

Buchsbaum, B. R., Greer, S., Chang, W.-L., & Berman, K. F. (2005). Meta-analysis of neuroimaging studies of the Wisconsin card-sorting task and component processes. *Human Brain Mapping*, *25*(1), 35–45.

Byrne, R. W., & Corp, N. (2004). Neocortex size predicts deception rate in primates. *Proceedings of the Royal Society. Series B: Biological Sciences*, *271*(1549), 1693–1699.

Carrión, R., Keenan, J., & Sebanz, N. (2009). A truth that's told with bad intent: An ERP study of deception. *Cognition*, *114*(1), 105–110.

Caso, L., Aldert, A. G., & Mann, V. S. (2005). Processes underlying deception: An empirical analysis of truth and lies when manipulating the stakes. *Journal of Investigative Psychology and Offender Profiling*, *2*(3), 195–202.

Chiu, P., Ambady, N., & Deldin, P. (2004). Contingent negative variation to emotional in- and out-group stimuli differentiates high- and low-prejudiced individuals. *Journal of Cognitive Neuroscience*, *16*(10), 1830–1839.

Christ, S., Van Essen, D., Watson, J., Brubaker, L., & McDermott, K. (2009). The contributions of prefrontal cortex and executive control to deception: Evidence from activation likelihood estimate meta-analyses. *Cerebral Cortex*, *19*(7), 1557–1566.

Clark, L., Blackwell, A. D., Aron, A. R., Turner, D. C., Dowson, J., Robbins, T. W., et al. (2007). Association between response inhibition and working memory in adult ADHD: A link to right frontal cortex pathology? *Biological Psychiatry*, *61*(12), 1395–1401.

Clark, L., Manes, F., Antoun, N., Sahakian, B. J., & Robbins, T. W. (2003). The contributions of lesion laterality and lesion volume to decision-making impairment following frontal lobe damage. *Neuropsychologia*, *41*(11), 1474–1483.

Damen, E., & Brunia, C. (1994). Is a stimulus conveying task-relevant information a sufficient condition to elicit a stimulus-preceding negativity? *Psychophysiology*, *31*, 129–139.

DePaulo, B. M., Lindsay, J. J., Malone, B. E., Muhlenbruck, L., Charlton, K., & Cooper, H. (2003). Cues to deception. *Psychological Bulletin*, *129*(1), 74–118.

Fabiani, M., Gratton, G., & Federmeier, K. D. (2007). Event-related potentials: Methods, theory, and applications. In J. T. Cacioppo, L. G. Tassinary, & G. G. Berntson (Eds.), *Handbook of psychophysiology* (3rd ed., pp. 85–119). New York, NY: Cambridge University Press.

Fang, F., Liu, Y., & Shen, Z. (2003). Lie detection with contingent negative variation. *International Journal of Psychophysiology*, *50*(3), 247–255.

Fassbender, C., Murphy, K., Foxe, J., Wylie, G., Javitt, D., Robertson, I., et al. (2004). A topography of executive functions and their interactions revealed by functional magnetic resonance imaging. *Cognitive Brain Research*, *20*(2), 132–143.

Fellows, L. K., & Farah, M. J. (2005). Different underlying impairments in decision-making following ventromedial and dorsolateral frontal lobe damage in humans. *Cerebral Cortex*, *15*(1), 58–63.

Floden, D., Alexander, M. P., Kubu, C. S., Katz, D., & Stuss, D. T. (2008). Impulsivity and risk-taking behavior

in focal frontal lobe lesions. *Neuropsychologia*, *46*(1), 213–223.

Ford, C. V., King, B. H., & Hollender, M. H. (1988). Lies and liars: Psychiatric aspects of prevarication. *American Journal of Psychiatry*, *145*(5), 554–562.

Fukui, H., Murai, T., Fukuyama, H., Hayashi, T., & Hanakawa, T. (2005). Functional activity related to risk anticipation during performance of the Iowa Gambling Task. *NeuroImage*, *24*(1), 253–259.

Furedy, J. J., Davis, C., & Gurevich, M. (1988). Differentiation of deception as a psychological process: A psychophysiological approach. *Psychophysiology*, *25*(6), 683–688.

Ganis, G., Kosslyn, S. M., Stose, S., Thompson, W. L., & Yurgelun-Todd, D. A. (2003). Neural correlates of different types of deception: An fMRI investigation. *Cerebral Cortex*, *13*(8), 830–836.

Garavan, H., Ross, T., & Stein, E. A. (1999). Right hemispheric dominance of inhibitory control: An event-related functional MRI study. *Proceedings of the National Academy of Sciences of the United States of America*, *96*(14), 8301–8306.

Garavan, H., Ross, T. J., Murphy, K., Roche, R. A. P., & Stein, E. A. (2002). Dissociable executive functions in the dynamic control of behavior: Inhibition, error detection, and correction. *NeuroImage*, *17*, 1820–1829.

Hala, S., & Russell, J. (2001). Executive control within strategic deception: A window on early cognitive development? *Journal of Experimental Child Psychology*, *80*(2), 112–141.

Johnson, J. R. (2006). Toward a neurocognitive basis of deception. *Journal of Credibility Assessment and Witness Psychology*, *7*(2), 41–46.

Johnson, J. R., Barnhardt, J., & Zhu, J. (2003). The deceptive response: Effects of response conflict and strategic monitoring on the late positive component and episodic memory-related brain activity. *Biological Psychology*, *64*(3), 217–253.

Johnson, J. R., Barnhardt, J., & Zhu, J. (2004). The contribution of executive processes to deceptive responding. *Neuropsychologia*, *42*(7), 878–901.

Johnson, J. R., Barnhardt, J., & Zhu, J. (2005). Differential effects of practice on the executive processes used for truthful and deceptive responses: An event-related brain potential study. *Cognitive Brain Research*, *24*(3), 386–404.

Johnson, J. R., Henkell, H., Simon, E., & Zhu, J. (2008). The self in conflict: The role of executive processes during truthful and deceptive responses about attitudes. *NeuroImage*, *39*(1), 469–482.

Knutson, B., Fong, G., Adams, C., Varner, J., & Hommer, D. (2001). Dissociation of reward anticipation and outcome with event-related fMRI. *NeuroReport*, *12*(17), 3683–3687.

Knutson, B., Fong, G., Bennett, S., Adams, C., & Hommer, D. (2003). A region of mesial prefrontal cortex tracks monetarily rewarding outcomes: Characterization with rapid event-related fMRI. *NeuroImage*, *18*(2), 263–272.

Konishi, S., Nakajima, K., Uchida, I., Kikyo, H., Kameyama, M., & Miyashita, Y. (1999). Common inhibitory mechanism in human inferior prefrontal cortex revealed by event-related functional MRI. *Brain*, *122*, 981–991.

Laird, A. R., McMillan, K. M., Lancaster, J. L., Kochunov, P., Turkeltaub, P. E., Pardo, J. V., et al. (2005). A comparison of label-based review and ALE meta-analysis in the Stroop task. *Human Brain Mapping*, *25*(1), 6–21.

Langleben, D. D., Loughead, J. W., Bilker, W. B., Ruparel, K., Childress, A. R., Busch, S. I., et al. (2005). Telling truth from lie in individual subjects with fast event-related fMRI. *Human Brain Mapping*, *26*(4), 262–272.

Langleben, D. D., Schroeder, L., Maldjian, J. A., Gur, R. C., McDonald, S., Ragland, J. D., et al. (2002). Brain activity during simulated deception: An event-related functional magnetic resonance study. *NeuroImage*, *15*(3), 727–732.

Lee, T. M. C., Au, R. K. C., Liu, H.-L., Ting, K. H., Huang, C.-M., & Chan, C. C. H. (2009). Are errors differentiable from deceptive responses when feigning memory impairment? An fMRI study. *Brain and Cognition*, *69*(2), 406–412.

Lee, T. M. C., Liu, H.-L., Chan, C. C. H., Ng, Y.-B., Fox, P. T., & Gao, J.-H. (2005). Neural correlates of feigned memory impairment. *NeuroImage*, *28*(2), 305–313.

Lee, T. M. C., Liu, H. L., Tan, L. H., Chan, C. C. H., Mahankali, S., Feng, C. M., et al. (2002). Lie detection by functional magnetic resonance imaging. *Human Brain Mapping*, *15*(3), 157–164.

Lewis, M., Stanger, C., & Sullivan, M. W. (1989). Deception in three-year-olds. *Developmental Psychology*, *25*(3), 439–443.

Leynes, P., Allen, J., & Marsh, R. (1998). Topographic differences in CNV amplitude reflect different preparatory processes. *International Journal of Psychophysiology*, *31*(1), 33–44.

Liddle, P., Kiehl, K., & Smith, A. (2001). Event-related fMRI study of response inhibition. *Human Brain Mapping*, *12*(2), 100–109.

Liu, X., Powell, D., Wang, H., Gold, B., Corbly, C., & Joseph, J. (2007). Functional dissociation in frontal and striatal areas for processing of positive and negative reward information. *Journal of Neuroscience*, *27*(17), 4587–4597.

Mostofsky, S., Schafer, J., Abrams, M., Goldberg, M., Flower, A., Boyce, A., et al. (2003). fMRI evidence that the neural basis of response inhibition is task-dependent. *Cognitive Brain Research*, *17*(2), 419–430.

Nieuwenhuis, S., Heslenfeld, D., Alting von Geusau, N., Mars, R., Holroyd, C., & Yeung, N. (2005). Activity in human reward-sensitive brain areas is strongly context dependent. *NeuroImage*, *25*(4), 1302–1309.

Owen, A., McMillan, K., Laird, A., & Bullmore, E. (2005). N-back working memory paradigm: A meta-analysis of normative functional neuroimaging studies. *Human Brain Mapping*, *25*(1), 46–59.

Scherg, M., & Ebersole, J. (1993). Models of brain sources. *Brain Topography*, *5*(4), 419–423.

Semlitsch, H. V., Anderer, P., Schuster, P., & Presslich, O. (1986). A solution for reliable and valid reduction of ocular artifacts, applied to the P300 ERP. *Psychophysiology*, *23*(6), 695–703.

Seth, A. K., Iversen, J. R., & Edelman, G. M. (2006). Single-trial discrimination of truthful from deceptive responses during a game of financial risk using alpha-band MEG signals. *NeuroImage*, *32*(1), 465–476.

Seymour, B., Daw, N., Dayan, P., Singer, T., & Dolan, R. (2007). Differential encoding of losses and gains in the human striatum. *Journal of Neuroscience*, *27*(18), 4826–4831.

Sip, K. E., Roepstorff, A., McGregor, W., & Frith, C. D. (2008). Detecting deception: The scope and limits. *Trends in Cognitive Sciences*, *12*(2), 48–53.

Spence, S. A. (2004). The deceptive brain. *Journal of the Royal Society of Medicine*, *97*(1), 6–9.

Spence, S. A., Farrow, T. F., Herford, A. E., Wilkinson, I. D., Zheng, Y., & Woodruff, P. W. (2001). Behavioural and functional anatomical correlates of deception in humans. *NeuroReport*, *12*(13), 2849–2853.

Spence, S. A., Hunter, M. D., Farrow, T. F. D., Green, R. D., Leung, D. H., Hughes, C. J., et al. (2004). A cognitive neurobiological account of deception: Evidence from functional neuroimaging. *Philosophical Transactions of the Royal Society. Series B: Biological Sciences*, *359*(1451), 1755–1762.

Spence, S. A., Kaylor-Hughes, C., Farrow, T. F. D., & Wilkinson, I. D. (2008). Speaking of secrets and lies: The contribution of ventrolateral prefrontal cortex to vocal deception. *NeuroImage*, *40*(3), 1411–1418.

Spencer, K., Dien, J., & Donchin, E. (2001). Spatiotemporal analysis of the late ERP responses to deviant stimuli. *Psychophysiology*, *38*(02), 343–358.

Stromwall, L. A., Granhag, P. A., & Landstrom, S. (2007). Children's prepared and unprepared lies: Can adults see through their strategies? *Applied Cognitive Psychology*, *21*(4), 457–471.

van Boxtel, G., & Böcker, K. (2004). Cortical measures of anticipation. *Journal of Psychophysiology*, *18*(2–3), 61–76.

Verleger, R., Wauschkuhn, B., van der Lubbe, R. H. J., Jaskowski, P., & Trillenberg, P. (2000). Posterior and anterior contribution of hand-movement preparation to late CNV. *Journal of Psychophysiology*, *14*(2), 69–86.

Vrij, A., & Mann, S. (2001). Telling and detecting lies in a high-stake situation: The case of a convicted murderer. *Applied Cognitive Psychology*, *15*(2), 187–203.

Walczyk, J. J., Roper, K. S., Seemann, E., & Humphrey, A. M. (2003). Cognitive mechanisms underlying lying to questions: Response time as a cue to deception. *Applied Cognitive Psychology*, *17*(7), 755–774.

Weerts, T., & Lang, P. (1973). The effects of eye fixation and stimulus and response location on the contingent negative variation (CNV). *Biological Psychology*, *1*(1), 1–19.